Available online at www.sciencedirect.com
SCIENCE DIRECT
Remote Sensing of Environment 97 (2005) 68 – 82
Remote Sensing of Environment
www.elsevier.com/locate/rse

Factors affecting remotely sensed snow water equivalent uncertainty

Jiarui Dong[a,b,*], Jeffrey P. Walker[c], Paul R. Houser[d]

[a]Hydrological Sciences Branch, NASA Goddard Space Flight Center, Code 974, Greenbelt, Maryland, 20771, USA
[b]Goddard Earth Sciences and Technology Center, University of Maryland Baltimore Country, Baltimore, Maryland, 21250, USA
[c]Department of Civil and Environmental Engineering, The University of Melbourne, Parkville, Victoria, 3010 Australia
[d]George Mason University & Center for Research on Environment and Water, Calverton, MD 20705-3106, USA

Received 22 October 2004; received in revised form 18 April 2005; accepted 24 April 2005

Abstract

State-of-the-art passive microwave remote sensing-based snow water equivalent (SWE) algorithms correct for factors believed to most significantly affect retrieved SWE bias and uncertainty. For example, a recently developed semi-empirical SWE retrieval algorithm accounts for systematic and random error caused by forest cover and snow morphology (crystal size — a function of location and time of year). However, we have found that climate and land surface complexities lead to significant systematic and random error uncertainties in remotely sensed SWE retrievals that are not included in current SWE estimation algorithms. Joint analysis of independent meteorological records, ground SWE measurements, remotely sensed SWE estimates, and land surface characteristics have provided a unique look at the error structure of these recently developed satellite SWE products. We considered satellite-derived SWE errors associated with the snow pack mass itself, the distance to significant open water bodies, liquid water in the snow pack and/or morphology change due to melt and refreeze, forest cover, snow class, and topographic factors such as large scale root mean square roughness and dominant aspect. Analysis of the nine-year Scanning Multichannel Microwave Radiometer (SMMR) SWE data set was undertaken for Canada where many in-situ measurements are available. It was found that for SMMR pixels with 5 or more ground stations available, the remote sensing product was generally unbiased with a seasonal maximum 20 mm average root mean square error for SWE values less than 100 mm. For snow packs above 100 mm, the SWE estimate bias was linearly related to the snow pack mass and the root mean square error increased to around 150 mm. Both the distance to open water and average monthly mean air temperature were found to significantly influence the retrieved SWE product uncertainty. Apart from maritime snow class, which had the greatest snow class affect on root mean square error and bias, all other factors showed little relation to observed uncertainties. Eliminating the drop-in-the-bucket averaged gridded remote sensing SWE data within 200 km of open water bodies, for monthly mean temperatures greater than −2 °C, and for snow packs greater than 100 mm, has resulted in a remotely sensed SWE product that is useful for practical applications.

Keywords: Snow water equivalent (SWE); Scanning Multichannel Microwave Radiometer (SMMR); Error analysis; Uncertainty

1. Introduction

Snow cover plays an important role in governing global energy and water budgets due to its high albedo, low thermal conductivity, and considerable spatial and temporal variability (Cohen, 1994; Hall, 1998). Moreover, model simulations demonstrate that local snow albedo feedbacks can enhance the North American climate anomalies related to El Nino-Southern Oscillation processes (Cohen & Entekhabi, 1999; Yang et al., 2001). Wintertime snow accumulation also has important springtime soil moisture implications that further enhance summer precipitation (Delworth & Manabe, 1998; Shukla & Mintz, 1982). Thus, accurate snow water equivalent (SWE) knowledge is important for short-term weather forecasts, climate change prediction, and hydrologic extreme (drought and flood) forecasting.

Space-borne passive microwave remote sensors, such as the Scanning Multichannel Microwave Radiometer (SMMR)

* Corresponding author. Hydrological Sciences Branch, NASA Goddard Space Flight Center, Code 974, Greenbelt, Maryland, 20771, USA.
E-mail address: jiarui@hsb.gsfc.nasa.gov (J. Dong).

0034-4257/$ - see front matter © 2005 Elsevier Inc. All rights reserved.
doi:10.1016/j.rse.2005.04.010

launched in 1978, provide a capability to monitor global scale SWE. Many investigators have carefully evaluated the quality of SMMR-derived snow depth data, and suggested good prairie region performance but poor boreal forest and high latitude tundra region performance (e.g., Robinson et al., 1993; Tait & Armstrong, 1996). To overcome these limitations, Foster et al. (2005) derived an alternate algorithm that made systematic error adjustments based on environmental factors such as forest cover and snow morphology (i.e. crystal size as a function of location and time of year).

The forest cover impact on remotely sensed SWE estimation is essentially a masking of the snow pack microwave emission by coniferous vegetation canopy biomass and the emission of vegetation canopy snow accumulation (Chang et al., 1996; Hall et al., 2002). Moreover, snow pack morphology affects the snow pack microwave emission by changing the crystal sizes. The snow pack morphology is strongly correlated with climate, and snow crystal size changes caused by temperature and water vapor gradients (Josberger & Mognard, 2002). Further, the wet snow microwave response is distinctly higher than dry snow microwave response for frequencies above 30 GHz, because water droplets absorb and reemit rather than scatter microwave radiation (Foster et al., 2005; Ulaby & Stiles, 1980). Previous studies have also suggested that complex topography within a large microwave footprint has a significant passive microwave SWE retrieval influence because of the difficulty in extracting snow signals (e.g., Matzler & Standley, 2000).

Understanding the retrieved SWE product uncertainty is critical for its successful utilization. While Foster et al. (2005) have developed an approach for quantitatively estimating SWE retrieval uncertainty based on error propagation theory, and have tested it with a Special Sensor Microwave Imager (SSM/I) retrieval error assessment for the period 1987 to present, the factors contributing to these errors are only best-guess estimates. This study makes a thorough uncertainty assessment of the Foster et al. (2005) semi-empirical SWE retrieval algorithm, relative to Canadian in-situ SWE measurements over the entire 9-year SMMR data set. The SMMR data is used for this analysis due to the greater SWE ground truth availability during that time period. We consider satellite-derived SWE errors associated with snow pack mass, distance to significant open water bodies, liquid water in the snow pack and/or morphology change due to melt and refreeze, forest cover, snow class, and topographic factors such as large scale root mean square roughness and dominant aspect.

2. Data

2.1. Passive microwave observations

There are currently several satellites that have made or are making passive microwave measurements at SWE-sensitive frequencies. These include: i) the Scanning Multi-channel Microwave Radiometer (SMMR) which is an imaging 5-frequency radiometer that was flown on the Seasat and Nimbus-7 Earth satellites, providing observations from October 25, 1978 to August 20, 1987 (Table 1); ii) the Special Sensor Microwave Imager (SSM/I) which is a passive microwave radiometer flown aboard Defense Meteorological Satellite Program (DMSP) satellites DMSP F-8, F-10, F-11, F-12, and F-13, providing observations from September 7, 1987 until present; and iii) the Advanced Microwave Scanning Radiometer for the Earth observing system (AMSR-E) which is a multi-frequency, dual-polarized microwave radiometer flown aboard NASA's Earth Observing System (EOS) Aqua platform, providing observations from May 2002 until present. This paper focuses on the 9-year SMMR data set that overlaps with more than 3000 Canadian SWE observation sites that are available during the 1980s and early 1990s, of which 1400 sites have at least 5 months of data for each winter season.

Several SWE estimation algorithms have been developed for passive microwave observations. The commonly used Chang et al. (1987) algorithm estimates SWE from the SMMR 18 and 37 GHz or SSM/I 19 and 37 GHz brightness temperature difference, multiplied by a constant derived from radiative transfer theory. The 37 GHz data is sensitive to snow pack scattering while the 18 GHz data is relatively unaffected by snow. Foster et al. (2005) have modified this algorithm using spatially and temporally varying constants that account for forest cover fraction and snow crystal size variations by

$$\mathrm{SWE} = F\ c\ (T_{18} - T_{37}), \tag{1}$$

where F is the fractional forest cover factor calculated using the International Geosphere-Biosphere Program (IGBP) land cover map described by Loveland et al. (2000), and c is parameterized according to the Sturm snow class categories (Sturm et al., 1995) and time of year. T_{18} and T_{37} are the horizontally polarized brightness temperatures at 18 GHz and 37 GHz respectively. Daytime SMMR observations and T_{37} observations greater than 240 K were excluded to minimize wet snow effects.

The SMMR instrument was cycled on and off every other day due to spacecraft power limitations (Njoku, 1996), decreasing the temporal resolution to more than 5 days. Thus, SMMR 5-day composites include overlapping high latitude observations and low latitude observation gaps. The

Table 1
Scanning Multifrequency Microwave Radiometer (SMMR) characteristics

Platform	Nimbus-7
Period of operation	October, 1978 to August, 1987
Data acquisition	Every other day
Swath width	780 km
Frequency (GHz)	6.6, 10.7, 18.0, 21 and 37
Footprint resolution (km)	55×41 (18 GHz)
	27×18 (37 GHz)
Polarization	H and V
Orbital timing (equator crossing)	Midday and midnight

recalibrated brightness temperature (T_b) data available for this study were obtained from the National Snow and Ice Data Center (NSIDC) Distributed Active Archive Center (DAAC) at the University of Colorado (Njoku, 1996) and had been processed onto a quarter-degree grid by using the drop-in-the-bucket method. Overlapping data in cells from different footprints on the same day were then averaged to give a single brightness temperature, assumed to be located at the center of the cell. Because SMMR footprint resolution at 18 GHz is 55 by 41 km, which approximates to the half-degree by half-degree resolution, it is more representative of the actual footprint size by averaging this quarter-degree data to half-degree. Fig. 1 shows an example of SMMR SWE estimates when using the Foster et al. (2005) algorithm for an individual 5-day nighttime composite. These composites were derived by first calculating SWE values for individual days and then averaging them over five consecutive days, taking into account times and locations where no data was observed.

2.2. In-situ snow observations

The Canadian Snow Water Equivalent Database (Brown, 1996) SWE estimates were derived from the Meteorological Service of Canada (MSC) daily snow depth observation network using an interpolated snow density from the snow survey network specifically designed to represent local terrain and vegetation. The resulting SWE estimates are reported to effectively represent observed spatial and temporal snow depth variability (Brown, 2000; Brown & Braaten, 1998; Mote et al., 2003).

The Canadian snow observations are quite spatially dense in the southern more populated regions and rather sparse further to the north (Fig. 2). There are 3701 observing stations with bi-weekly recordings from the mid-1950s to the mid-1990s, with a pronounced active recording station peak from 1980 to 1995. During the latter-half of the 1990s, the number of active reporting stations declined by more than 25% (Brown et al., 2003). The number of active reporting stations is quite dynamic, making the observation record length highly variable during the 1979 to 1987 SMMR timeframe. For example, 638 stations have no data, and only 227 stations have complete data for the entire SMMR time period (Fig. 2a). Different length in-situ station records are combined to give an average SMMR SWE error estimate over the observing interval, so it is important to note that some results may be impacted by interannual variability.

There is a recognized spatial discrepancy between the in-situ observing station point measurements and the half-degree by half-degree SMMR footprint (or pixel) SWE estimates. Chang et al. (2005) suggested that 10 distributed

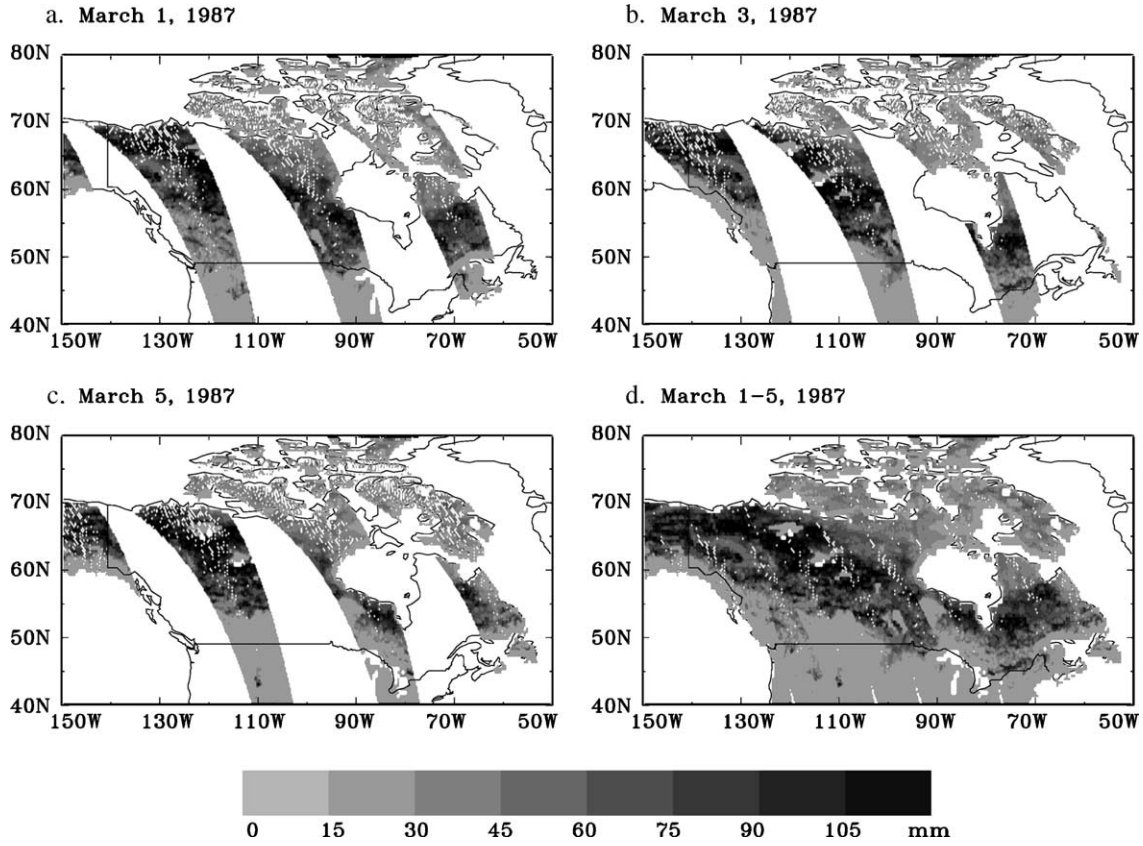

Fig. 1. An SMMR passive microwave SWE estimate for three consecutive nighttime overpasses on (a) March 1, (b) March 3, and (c) March 5, 1987, and (d) the 5-day observation composite.

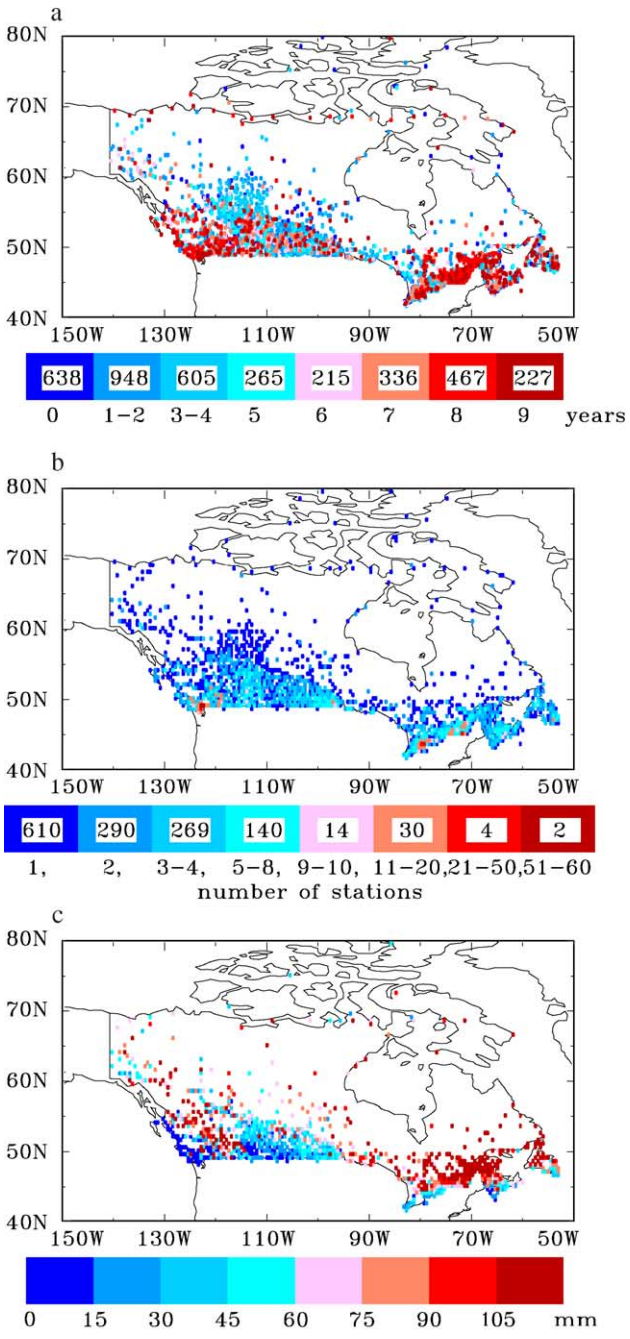

Fig. 2. In-situ SWE spatial and temporal station characteristics: (a) data set length during the 1979 to 1987 period — the numbers in the color bar show how many stations have the indicated data length; (b) number of stations in each half-degree grid cell — numbers in the color bar show the number of grid cells with the indicated number of stations; (c) the 1979 to 1987 average winter season in-situ SWE data averaged to half-degree grid cells.

snow depth measurements per one-degree by one-degree grid cell are required to produce a sampling error of 5 cm or better. To minimize this discrepancy, we average in-situ station SWE measurements to half-degree by half-degree (approximately 50 km by 35 km at 50°N) pixels, which results in 1359 pixel averages with 1 or more stations and 802 pixel averages covering 1 or more years. The number of observing stations available for each SMMR half-degree pixel varied widely, ranging from 1 to 60 (Fig. 2b). However, most SMMR pixels contain fewer than 5 stations, with only 190 having more than 5 stations. Although northern Canada has few stations, they still provide valuable uncertainty information for a broader environmental condition range. Fig. 2c shows the 1979 to 1987 average winter season in-situ SWE data averaged to the half-degree pixels.

3. Error assessment

The SMMR retrieved SWE uncertainty relative to in-situ observations is investigated using root mean square (RMS) error, relative RMS (RRMS) error, bias (BIAS) and relative bias (RBIAS) measures. The BIAS is defined as the difference between satellite and in-situ data. The RRMS and RBIAS are defined as the RMS or BIAS of a given half-degree pixel divided by the pixel mean SWE across the SMMR 9-year timeframe. These relative calculations are made using both the SMMR (subscript SMMR) and in-situ observations (subscript OBS) SWE estimates.

The error statistics are calculated for the 1359 half-degree pixels with coincident ground truth observations, for the winter seasons (November to April) during the period of 1979 to 1987. The left column in Fig. 3 shows the RMS error statistics spatial distribution. The most eastern regions and some mountainous areas show the largest RMS errors with values above 200 mm. The west near-coastal regions have very small RMS errors with values below 25 mm. This is due to this region's lower snow amounts, which is illustrated by the $RRMS_{OBS}$ error statistic that normalizes for mean ground SWE amounts. These errors are over 200% in most west coast regions and some isolated east coast locations; errors are also above 100% in most of south-eastern Canada, particularly near the Great Lakes and in western mountainous areas. There are similar patterns found in the $RRMS_{SMMR}$ errors statistic, but the error values are much larger due to the general SMMR SWE underestimation (Fig. 3e).

The right column in Fig. 3 shows the corresponding winter average bias errors (BIAS, $RBIAS_{OBS}$ and $RBIAS_{SMMR}$) during the 1979 to 1987 period. Most regions show a SMMR SWE underestimation, except for a few prairie and taiga stations (refer to Fig. 5e) with overestimation of less than 20 mm. Similarly, most eastern regions and some mountainous area SMMR SWE estimates are biased high, with some areas having more than a 50 mm underestimation (Fig. 3b). Both east and west near-coastal regions and regions near the Great Lakes have very small bias errors with values below 50 mm, but their relative biases are large, with $BIAS_{OBS}$ above 75% and $BIAS_{SMMR}$ above 500% underestimation (Fig. 3d and f). RMS error estimates reflect both bias errors and random errors. Fig. 4a shows that a large component of the RMS error is contributed from bias, with most stations in the west

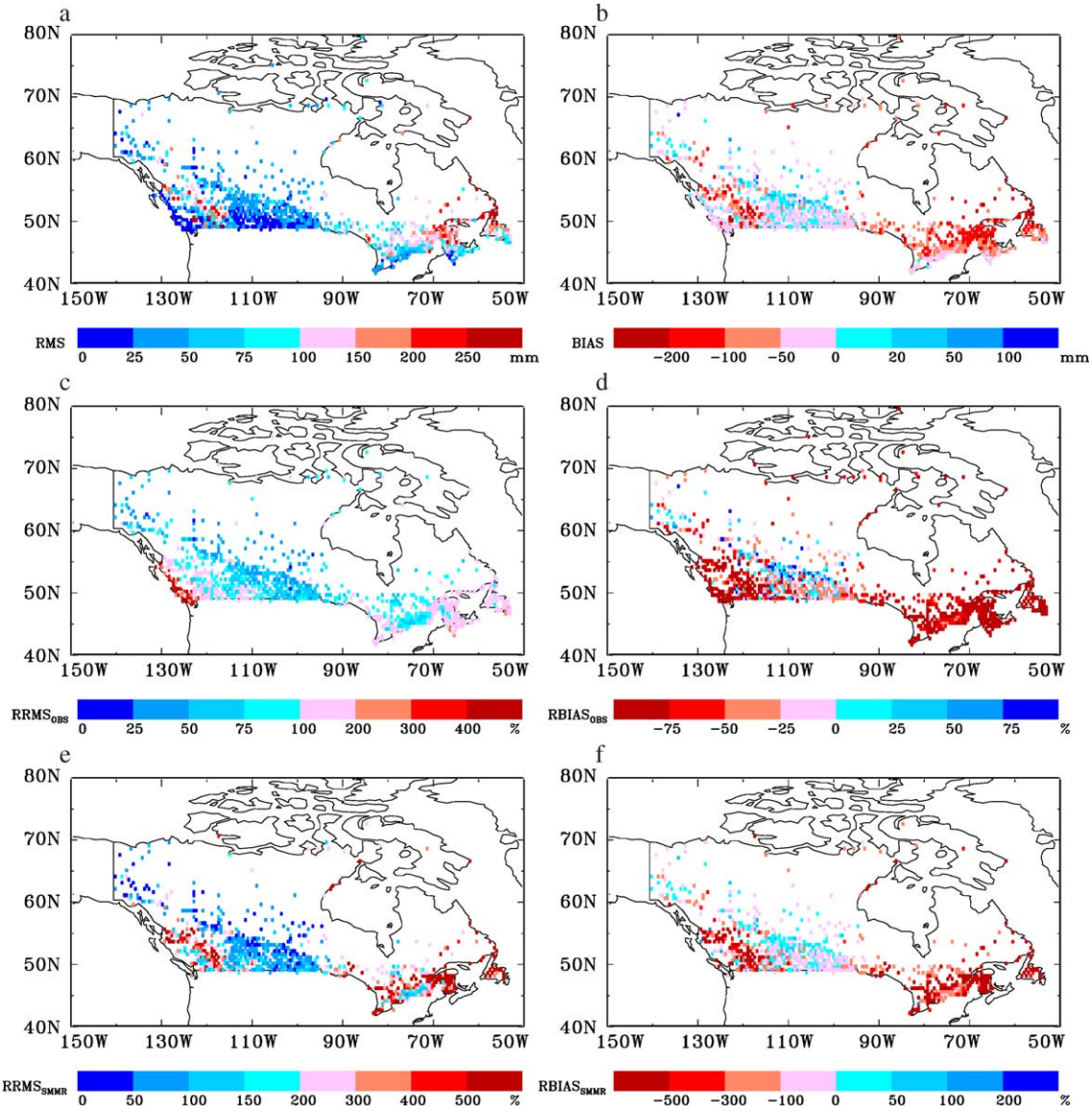

Fig. 3. Half-degree SMMR passive microwave SWE retrieval error statistics for pixels with coincident half-degree ground truth station data: (a) root mean square (RMS) error, (b) bias (BIAS) error, (c) root mean square errors relative to the ground truth measurements ($RRMS_{OBS}$), (d) bias errors relative to the ground truth measurements ($RBIAS_{OBS}$), (e) root mean square errors relative the SMMR estimates ($RRMS_{SMMR}$), and (f) bias errors relative to the SMMR estimates ($RBIAS_{SMMR}$).

mountainous regions and east of 95°W having more than 70% contribution of bias to the RMS error. The bias contributions are smaller on the west coast, east coast below 50°N, and most prairie regions.

To ascertain what might be contributing to the spatial variability of SMMR SWE error, a comparative analysis with several environmental variables was undertaken. The obvious tendency for higher error near significant water bodies shown in Fig. 3 results from free water molecules significantly increasing the brightness temperature at 37 GHz by emission rather than microwave energy scattering (Foster et al., 2005), which can produce significant retrieval contamination more than 100 km from the water body due to the footprint intersection or/and signal mixing (Bellerby et al., 1998). Fig. 4b compares the SMMR SWE seasonal bias with distance to the nearest five significant water bodies, defined as oceans, the Great Lakes, small lakes, Hudson Bay and water surrounding the northern Canadian islands.

Considering the effects from the projection distortion, the distances to nearest water body (D in kilometers) is calculated as:

$$D = \frac{R\pi}{180} \times \sqrt{\left[(\mathrm{Lon}_{\mathrm{obs}} - \mathrm{Lon}_{\mathrm{water}})\cos\left(\frac{\mathrm{Lat}_{\mathrm{obs}} + \mathrm{Lat}_{\mathrm{water}}}{2} \cdot \frac{\pi}{180}\right)\right]^2 + (\mathrm{Lat}_{\mathrm{obs}} - \mathrm{Lat}_{\mathrm{water}})^2}, \quad (2)$$

where R is the earth radius (6371 km), $\mathrm{Lat}_{\mathrm{obs}}$ and $\mathrm{Lon}_{\mathrm{obs}}$ represents the latitude and longitude at each in-situ station (in unit of degree), and $\mathrm{Lat}_{\mathrm{water}}$ and $\mathrm{Lon}_{\mathrm{water}}$ represents the

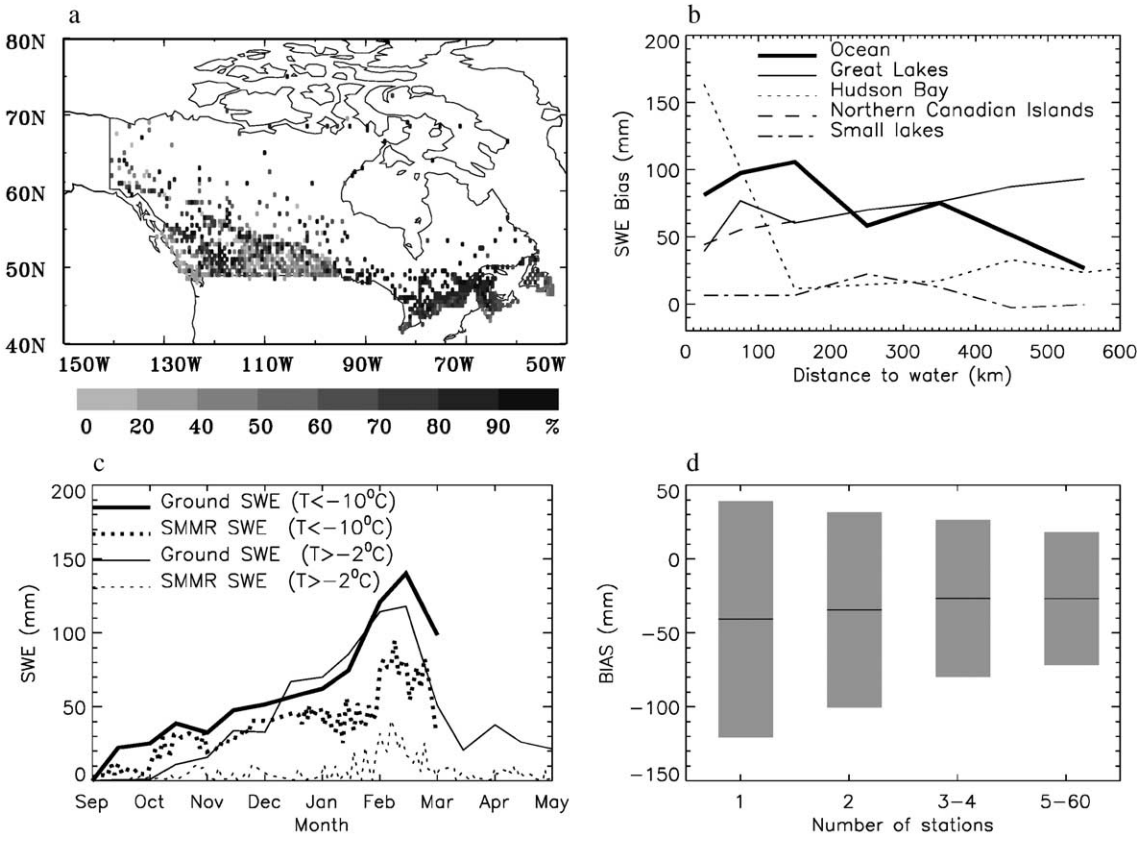

Fig. 4. Key SMMR passive microwave SWE retrieval error characteristics relative to the in-situ SWE observations: (a) the bias error to RMS error ratio, (b) mean bias of SWE relative to distance from five different water bodies, (c) comparison of monthly mean SWE from SMMR and station data for all ground truth pixels with monthly mean air temperature above and below indicated thresholds, and (d) the mean biases (lines) and their standard deviations (bar) calculated from the individual bias estimates of all pixels with a given number of stations.

latitude and longitude at the center of the nearest water pixel (in unit of degree). Doing this analysis on a half-degree grid may distort the results by up to a quarter-degree (half pixel), which is from the water pixel centroid to land.

There was no obvious influence from the small inland lakes and Hudson Bay, which likely results from their freezing and becoming snow covered during the winter months. In contrast, the SMMR SWE data showed significant coastal region underestimation with the mean bias reaching about 100 mm. This is because the oceans freeze only at much colder temperatures, so they do not become snow covered like the Hudson Bay and inland lakes. The Great Lakes and water surrounding the northern Canadian islands resulted in about 50 mm of underestimation. This intermediary level of bias may result from late freezing in the Great Lakes and ice effects (see Grody & Basist, 1997; West et al., 1996) in the north. Generally, there is a large SWE bias for regions close to large open water bodies.

Free water and ice interact with microwave energy very differently from snow crystals (Derksen et al., 2000). Therefore, we consider the potential for snowmelt, the presence of liquid water in the snow pack, or the subsequent snow pack refreezing, as inferred from daytime air temperature. A gridded half-degree monthly mean and diurnal range temperature product generated by interpolating directly from station observations was used for this purpose (New et al., 2000). Fig. 4c compares the seasonal SMMR SWE variation with the in-situ observations for daytime air temperatures above −2 °C and below −10 °C respectively, to highlight two extreme temperature range effects. A close agreement was found between the remotely sensed and in-situ SWE for temperatures below −10 °C, with some deep snow pack underestimation caused by passive microwave signal saturation. However, for temperatures close to or above freezing, there was a significant SMMR SWE underestimation with the largest difference reaching 100 mm. This is largely because wet snow and refreezing ice significantly raise the 37 GHz microwave brightness temperature.

Finally, to ascertain the in-situ sampling density effect within SMMR pixels, the mean bias errors and standard deviation (calculated from the individual bias estimates of all pixels with a given number of stations) have been plotted against number of stations per pixel (Fig. 4d). The mean bias is calculated as the average of bias estimates for all pixels. The mean bias errors show the improvement from more than 40 mm SWE underestimation for pixels with only 1 station to less than 30 mm SWE underestimation for pixels with 5 or more stations, and the corresponding mean

standard deviations decrease from 80 to 45 mm. The most likely reason for this improvement is that the increased number of stations yields an areal average estimate that is more compatible with the remote sensor. Therefore this analysis separately plots data for pixels with 5 or more stations.

These findings lay the foundation to explore the distance from water, air temperature, and related environmental factor impact on passive microwave SWE retrieval error.

4. Error exploration

4.1. Environmental factors

We have analyzed the potential passive microwave SWE retrieval error contribution from many environmental factors, including air temperature, distance to large open water bodies, snow class, forest cover, and topographic factors such as large-scale root mean square roughness and

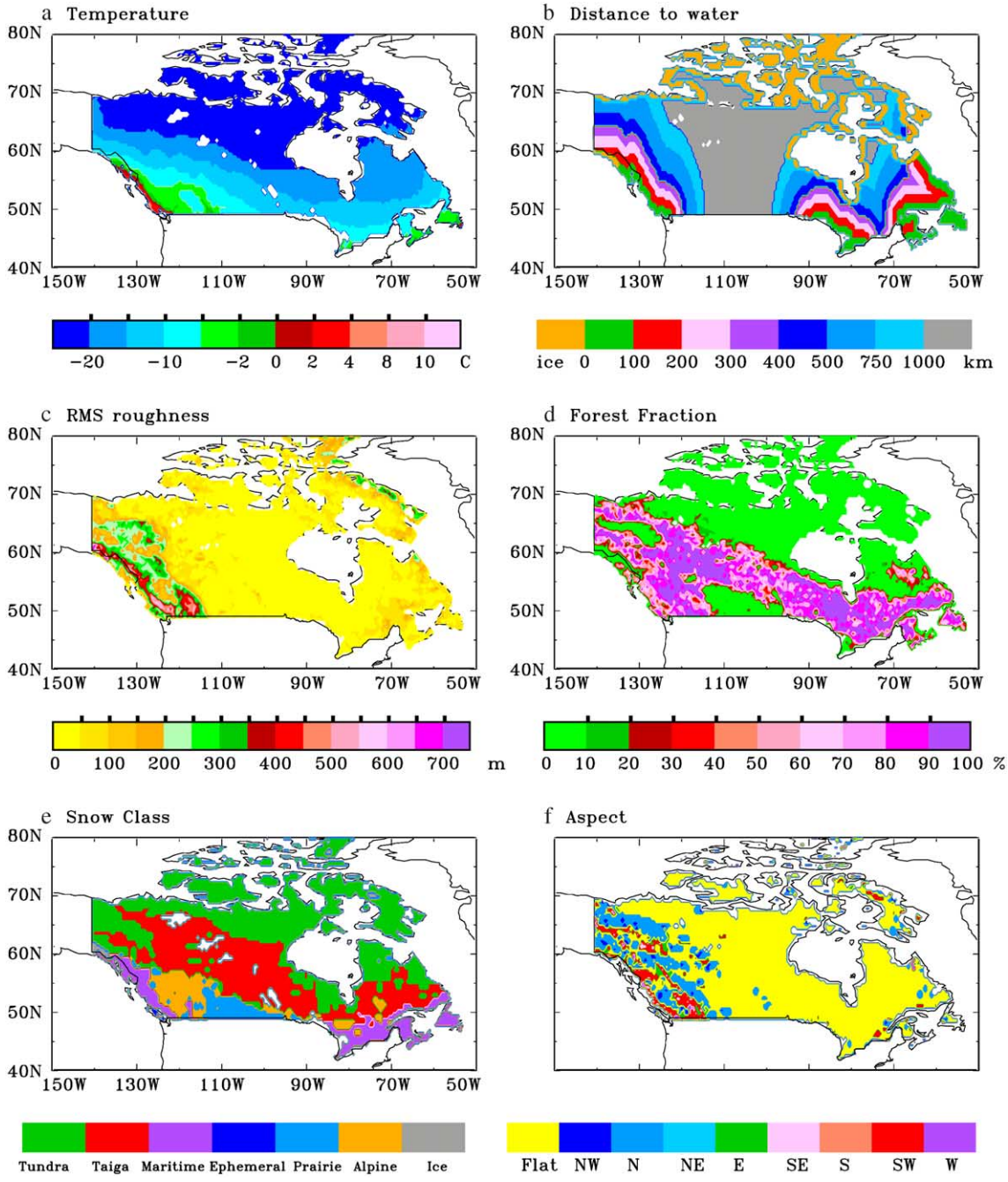

Fig. 5. Spatial maps of the environmental variables used in the SMMR passive microwave SWE retrieval error analysis: (a) average January air temperature, (b) distance to ocean water and Great Lakes-ice effects are considered for Hudson Bay and northern Canadian waterways due to winter freezing, (c) half-degree ground pixel root mean square roughness, (d) half-degree ground pixel fractional forest cover used in the satellite retrieval algorithm, (e) Sturm snow class used in the satellite retrieval algorithm, and (f) half-degree dominant topographic aspect.

dominant aspect (Fig. 5). Air temperature and distance to water were considered for the reasons outlined above. Snow class and forest factor were considered as they are key inputs to the SWE algorithm and have been previously shown to impact SWE estimation accuracy (Matzler & Standley, 2000). The snow class indicates snow crystal size by climate and season, which controls the passive microwave scattering signal emitted by the snow surface. The forest factor indicates forest cover fraction, which can mask the underlying snow pack microwave signal. Roughness controls microwave signal scattering, but only large-scale topographic roughness (rather than micro-roughness) was considered because it was believed to be more relevant at the passive microwave footprint scale, and because micro-roughness information is not available. Topographic aspect potentially interacts with the sensor's incidence angle, thereby masking the lee side of steep topography. The SMMR sensor was forward looking with a 50.3° along track incidence angle (Madrid, 1978), indicating that northwest and southeast facing slopes are most likely to have aspect-related errors, which are not considered by the SMMR SWE retrieval algorithm. Because RMS error for a given month in each pixel is calculated through a 9-year period sampling, the large seasonal temperature variability rather than the interannual variability is considered in the error statistic calculation across the 9-year SMMR time period. Fig. 5a shows an example of monthly (January) average temperature data derived from the 1979 to 1987 station observations.

Based on the foregoing analysis, we treated the water body effects on SWE passive microwave retrieval as follows (Fig. 5b). For open water bodies such as the Great Lakes and Oceans, distance to water is simply the distance to the closest open water body due to their infrequent wintertime freezing. Other water bodies were given the following special treatment: i) small lakes are assumed frozen and therefore are ignored; and ii) the effects of Hudson Bay and northern Canadian waterways are considered to be moderate, extending inland not more than 100 and 200 km respectively due to their wintertime freezing. The oceans show the most significant correlation with SWE retrieval errors, showing 100 mm underestimates within 200 km and dropping to about 30 mm underestimates beyond 500 km.

Large-scale roughness and aspect (Fig. 5c and f) were derived at half-degree resolution based on the GTOPO30 global 30-s digital elevation model (Gesch & Larson, 1996). Roughness was calculated as the root mean square of the elevation difference relative to the mean pixel elevation, and aspect was defined as the normal direction of the maximum slope between a half-degree pixel and its eight neighbors for elevation differences greater than 200 m.

Half-degree resolution IGBP forest fraction derived from 1 km satellite-based land cover data (Loveland et al., 2000) were used to investigate the overlying forest canopy masking effects on snow pack microwave emission (Fig. 5d). Forest fraction is the fraction of each half-degree pixel area occupied by forest land covers (including broadleaf forests, needleleaf forests, mixed forests, woodland, and half the area covered by wooded grassland). Comparison of total forest area estimates from inventory and remote sensing data provides some confidence in the remotely sensed forest fraction data (Dong et al., 2003).

The physically based Sturm et al. (1995) snow classification (Fig. 5e) differentiates snow packs based on typical snow layer sequence, thickness, density, crystal morphology and grain characteristics. The six resulting snow classes are Tundra, Taiga, Prairie, Alpine, Maritime, and Ephemeral.

4.2. Effects of environmental factors

The relationship between the average winter season RMS error and bias and the average monthly daytime temperature, distance to water, RMS roughness, forest fraction, snow class, aspect, and snow pack mass are shown in Figs. 6 and 7. The errors relative to SMMR estimates and ground observations are also shown. The snow pack mass has a significant relationship with passive microwave SWE estimate error, especially for SWE above 100 mm. Due to microwave signal saturation, the SMMR SWE algorithm is unable to reliably retrieve SWE for snow packs deeper than 150 mm, showing 100% relative RMS errors (Fig. 6a) that mostly result from a relative 90% SWE underestimation bias (Fig. 7a). However, RMS errors were small when excluding SWE values greater than 100 mm, with the relative SWE underestimation bias being reduced to less than 70%. Most pixels with 5 or more in-situ stations have SWE values less than 100 mm and show lower, nearly unbiased RMS errors (crosses in Figs. 6 and 7). Therefore, the sampling density has significant implications on the comparison between in-situ and remotely-sensed SWE observations.

There is an obvious nonlinear relationship between the relative RMS ($RRMS_{OBS}$) errors and both distance to water and temperature (Fig. 6b3 and c3). Errors consistently decrease for cold climate stations far from water, and sharply increase for warm climate stations close to open water.

Snow properties are season and climate dependent, reflecting the temperature during and after accumulation, the precipitation or condensation rate, and wind history (Sturm et al., 1995). Therefore, air temperature is potentially a major passive microwave SWE retrieval uncertainty indicator. Air temperature changes will significantly influence snow structures (density and crystal size), and thus alter the microwave emission. An air temperature close to or above 0 °C is a good indicator of liquid water in the snow pack, which dramatically reduces the snow pack's microwave volume scattering. Although the RMS error and bias are lower than 50 mm (Figs. 6b and 7b), there are larger relative RMS errors in these high temperature regions, which are partly contributed from the increasing bias errors. The mean relative bias underestimation increases from less

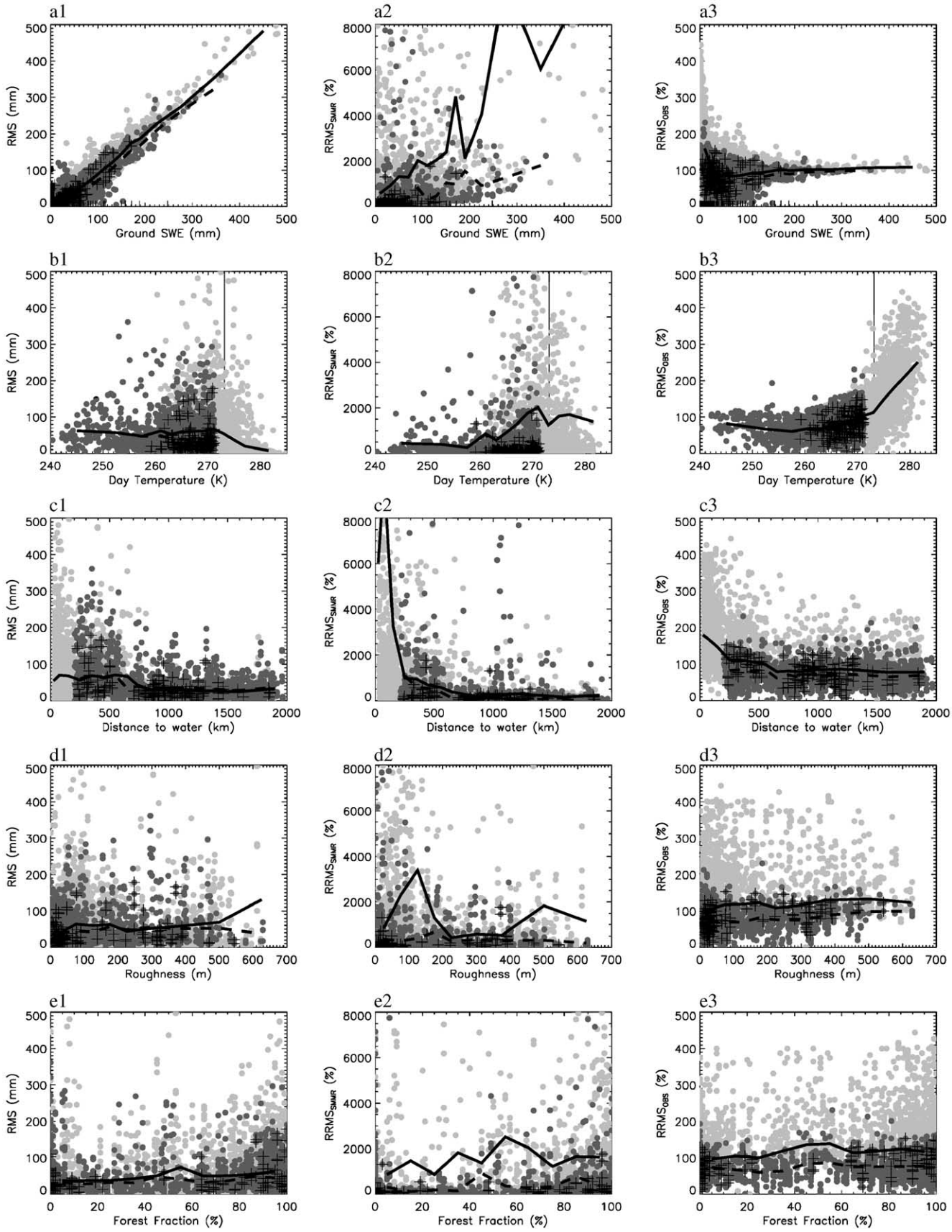
a1
a2
a3
RMS (mm)
RRMS$_{SMMR}$ (%)
RRMS$_{OBS}$ (%)
Ground SWE (mm)
b1
b2
b3
Day Temperature (K)
c1
c2
c3
Distance to water (km)
d1
d2
d3
Roughness (m)
e1
e2
e3
Forest Fraction (%)

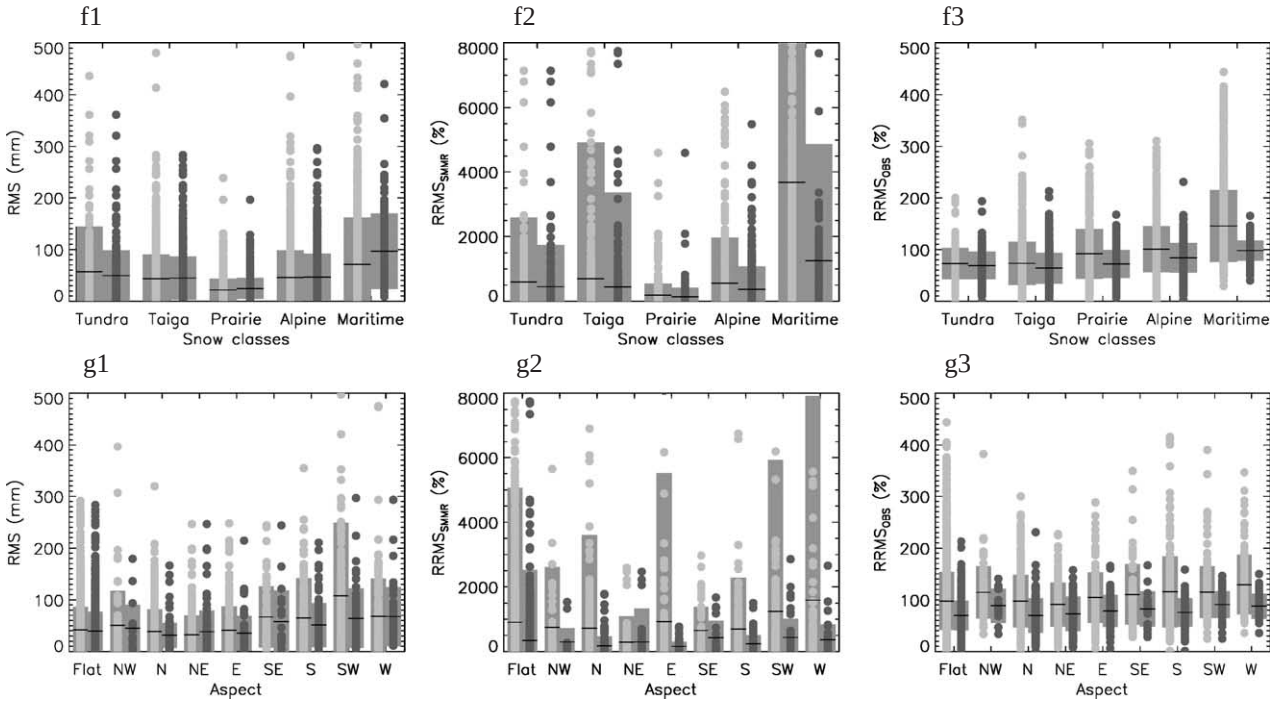

Fig. 6. SMMR passive microwave SWE retrieval root mean square (RMS) error (column 1), root mean square error relative to SMMR ($RRMS_{SMMR}$) estimates (column 2), and root mean square error relative to ground truth station ($RRMS_{OBS}$) data (column 3), shown relative to the in-situ SWE estimates (row a), average monthly daytime temperature (row b), "distance" to water (row c), RMS roughness (row d), forest fraction (row e), snow class (row f) and ground pixel aspect (row g). The light grey dots show all the data and dark gray dots show the data remaining after omitting pixels closer than 200 km to water and with an average monthly daytime temperature above −2 °C; the lines show the mean values respectively. The pluses represent data for pixels including 5 or more ground stations and the "boxes" (rows f and g) show plus and minus one standard deviation.

than 10% at −20 °C to over 40% above 0 °C. Because the SMMR SWE estimates derived for a melting snow pack are significantly underestimated and generally unreliable, we omit all data with a monthly daytime air temperature greater than −2 °C. Pixels with 5 or more stations are generally located in warm regions with mean temperatures above −10 °C. The randomly distributed relative bias at a range from 0 to 100% with nearly unbiased errors suggest that RMS errors for these pixels mostly result from the seasonal snow mass variability rather than the systematic bias between pixel SMMR SWE estimates and in-situ point observations.

Large passive microwave SWE retrieval errors are found within approximately 200 km of open water that decrease with distance from water (Figs. 6c and 7c). At approximately 200 km from open water, the SWE retrieval error sharply decreases with only slight decreases beyond 200 km. As open water bodies are obviously severely contaminating the passive microwave, we omit all data within 200 km of significant open water bodies in our subsequent analysis. Even after the temperature and distance to water truncations, some larger RMS errors are still evident that we speculate are related to mountainous terrain or inland lakes; we have not attempted to remove these SMMR pixels from this analysis.

SMMR SWE errors related to topographic roughness and aspect are almost exclusively confined to the western Canadian mountain areas, as the central and eastern Canadian landscape is relatively flat (Fig. 5c and f). There are slight increases in relative RMS_{OBS} errors and relative bias errors associated with increasing surface roughness (Figs. 6d and 7d), but the RMS errors and bias do not show any obvious trend, and the omitted data distribute randomly in different roughness ranges. Generally, the southerly and westerly facing slopes have slightly larger RMS and bias errors than the northerly and easterly facing slopes, with southwest facing slopes having the largest error (mean RMS error above 100 mm and mean bias about 90 mm underestimation). However, the relative RMS and bias errors do not show much difference among different aspects (Figs. 6g and 7g). As topographical factors do not show obvious SMMR SWE retrieval contamination, topographical correction is not pursued further in this analysis.

After omitting data with large water and air temperature related errors, relative SMMR SWE RMS and bias errors do not show any obvious trend with increasing forest fraction factor (Figs. 6e and 7e), but some stations with large forest fraction do have large RMS errors and bias. Again the omitted data distribute randomly amongst the different forest fraction ranges. The lowest errors were found in the Prairie snow class, with the largest mean error in the Maritime class (Figs. 6f and 7f). It was observed that Maritime class mean relative RMS and bias errors were reduced by nearly 50% and 10% respectively after the water

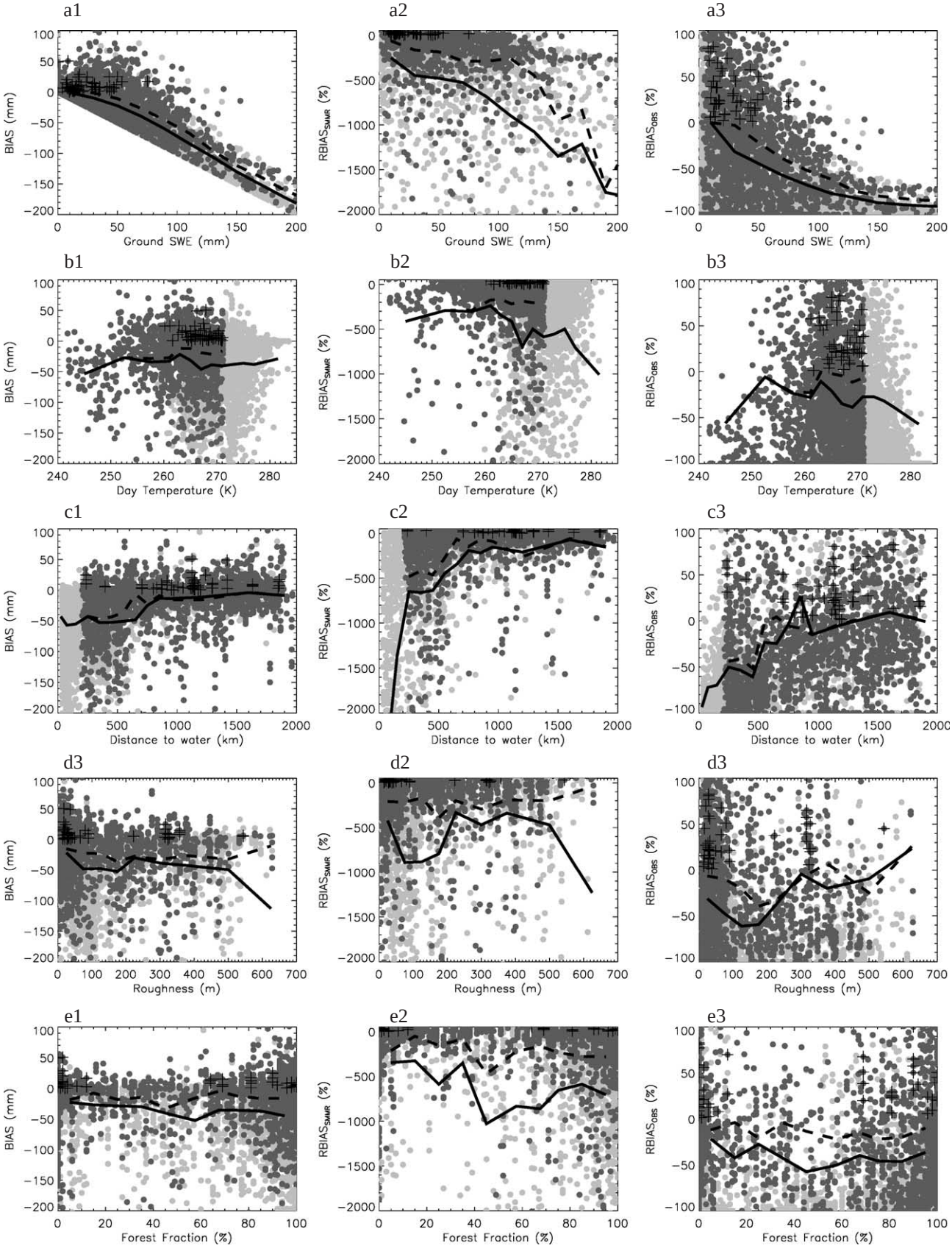

Fig. 7. As for Fig. 6 but for bias (SMMR-OBS) rather than RMS error.

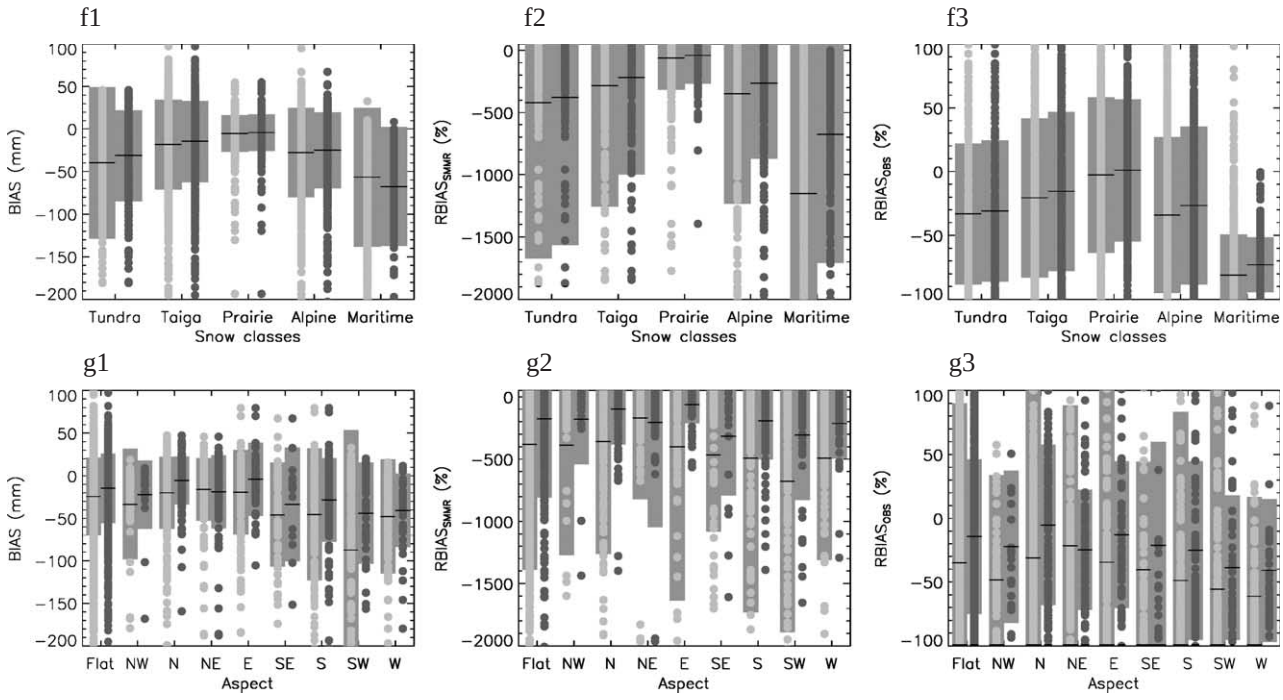

Fig. 7 (*continued*).

and temperature related omissions, owing to the Maritime class being in warmer climates near open water bodies (Fig. 5e). The errors from pixels with 5 or more in-situ stations are randomly distributed beyond 200 km from the open water and have different roughness and forest fractions (Figs. 6c–e and 7c–e). Therefore, either the forest cover and snow crystal size related SWE errors are small or are mitigated by the Foster et al. (2005) retrieval algorithm, so additional forest cover and snow crystal size corrections are not considered.

Foster et al. (2005) estimates SWE retrieval errors based on standard error propagation theory, without fully substantiating the contributing error factors. Their predicted SWE errors are significantly underestimated as compared to SMMR SWE error estimated from the observed Canadian in-situ SWE observations (Fig. 8). However, it is encouraging that the seasonal variations are in a good agreement with the observed mean RMS. Therefore, the Foster et al. (2005) vegetation cover and snow crystal related SMMR SWE retrieval error estimation approach may be reasonable, but their best-guess estimates of parameter uncertainty need to be updated with rigorously determined estimates from field campaigns and in-situ observations.

5. Error mitigation and application

This study shows that many factors contribute to passive microwave SWE retrieval error, and that ground data are limited by spatial representativeness and spatial and

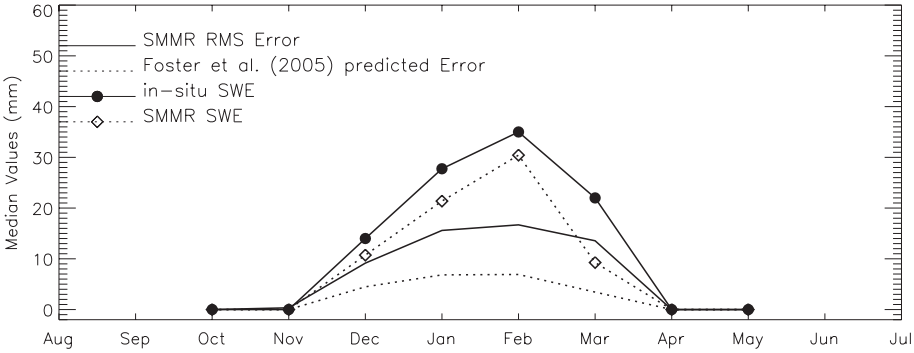

Fig. 8. Monthly average RMS median error of SMMR SWE retrievals, Foster et al. (2005) predicted error, in-situ SWE, and SMMR SWE estimates for pixels farther than 200 km from open water, with an average monthly daytime temperature below −2 °C, an in-situ SWE value of less than 100 mm, and only for pixels with 5 or more ground stations.

temporal availability. Thus remote sensing is the only practical global SWE mapping solution. However, practical SWE remote sensing application requires both a valid SWE retrieval error estimate and acceptably low retrieval errors. To eliminate the largest SMMR SWE errors, we propose that retrievals should be omitted for i) regions within 200 km of significant open water bodies, ii) times when monthly average air temperature is greater than −2 °C, and iii) times and locations where SWE values are above 100 mm as the SMMR SWE algorithm becomes insensitive. This results in an unbiased SMMR SWE estimate whose RMS median error varies through the season with a 20 mm seasonal maximum when comparing pixels with 5 or more stations (Fig. 8).

The monthly RMS median error of SMMR SWE retrievals in Fig. 8 was obtained by first calculating the RMS error in each pixel over the 9-year period and then obtaining the median among the pixels including 5 or more in-situ stations, while Foster et al. (2005) predicted errors were based on standard error propagation theory with empirically assigned contributing error factors for each ten percentile of fractional forest cover and different snow classes. The largely overlapping SMMR SWE and in-situ SWE seasonal standard deviation ranges allow for the filtered SMMR SWE estimate to be considered unbiased (Table 2). The seasonally-varying SMMR SWE median error is a function of the SMMR SWE algorithm's reduced sensitivity with increasing snowpack mass. While these recommendations are specific to the Foster et al. (2005) SMMR SWE retrieval, they may be generally applicable to all passive microwave SWE estimates with revised distance to water and temperature cut-off criteria.

Only omitting data within a narrow coastal region can significantly reduce the errors in regions with temperature above −10 °C, and only omitting data in regions with temperature above −2 °C reduces the errors beyond the coastal regions (Figs. 6b,c and 7b,c). By performing the two omissions simultaneously, the relative errors related to other environmental factors are reduced significantly (Figs. 6a3–g3 and 7a3–g3). The relative RMS errors related to roughness are reduced about 40%, including a 20% reduction for the relative bias errors (Figs. 6d3 and 7d3). The bias related to southwestern facing slopes is reduced from a 90 mm underestimation to below 50 mm (Fig. 7g1), and the bias related to forest fraction is reduced more than 20% (Fig. 7e1 and e3).

Table 2
Monthly average RMS median error and standard deviation of in-situ and SMMR SWE estimates for pixels farther than 200 km from open water, with an average monthly daytime temperature below −2 °C, an in-situ SWE value of less than 100 mm, and only for pixels with 5 or more ground stations (as used in Fig. 8)

	Median values (mm)		Standard deviation	
	In-situ	SMMR	In-situ	SMMR
October	0.0	0.0	0.0	0.1
November	0.0	0.0	5.4	3.9
December	14.0	10.7	15.0	11.9
January	27.8	21.4	21.0	16.5
February	35.0	30.4	23.4	18.6
March	22.0	9.3	24.7	16.8
April	0.0	0.0	9.1	2.8
May	0.0	0.0	1.2	0.6

The SMMR SWE error related to open water contamination was found to vary with distance from water, but not with time. In contrast, SMMR SWE retrieval error relative to air temperature was found to vary both spatially and temporally. Fig. 9 shows how much SMMR data are actually eliminated in order to mitigate the SMMR passive microwave SWE retrieval error caused by distance to water and monthly average daytime temperature. For each pixel, we first consider the effect from open water and then consider the effect from air temperature beyond the coastal regions. Omitting SMMR SWE retrievals for regions within 200 km of significant open water bodies results in about 5% reduction of the SMMR data set with varying fractions indicating different satellite tracks from month to month. In practical applications, the actual monthly average air temperature should be used. The omission of SMMR SWE data for times when monthly average daytime air temperature is above −2 °C significantly reduces the SMMR data set coverage in early spring. With the exception of coastal areas, reliable SMMR SWE retrievals should be available for most regions in November, December, January, February, and March for most years, with reduced areas in April, May, and October, and also March in some years (e.g., in year 1980–1981) owing to relatively high temperatures.

6. Conclusions

This study has used independent ground-based snow water equivalent observations to investigate remotely sensed passive microwave SWE estimation uncertainty related to snow pack mass, distance to significant open water bodies, daytime air temperature, forest cover, snow class, and topographic roughness and aspect. The passive microwave SWE retrieval error was dominated by the snow pack mass, with secondary factors being the distance to open water and air temperature. The SMMR SWE retrievals are sensitive to mixed pixels that include unfrozen open water for distances of up to 200 km from the open water. Daytime air temperature above −2 °C were also found to be related to satellite SWE retrieval uncertainty due to physical warm condition snow pack structure and crystal size changes and the presence of liquid water in the snow pack. Apart from the maritime snow class, the other environmental variables assessed had only slight relationships with satellite SWE retrieval uncertainty. Omitting the drop-in-the-bucket averaged gridded SMMR SWE retrievals for regions within 200 km of significant open water bodies, air temperatures above

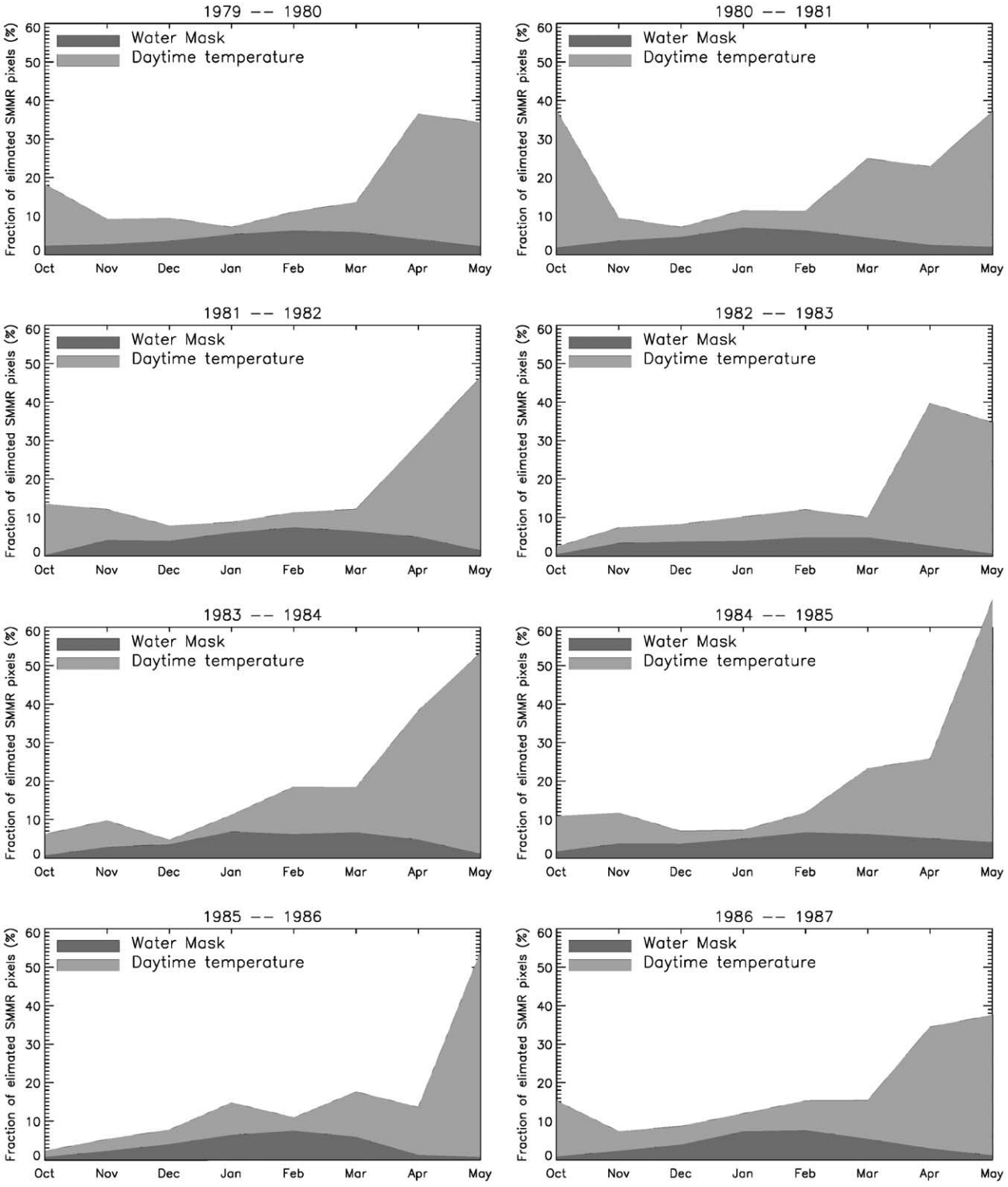

Fig. 9. Fraction of SMMR SWE retrievals eliminated in snow season (October to May) from 1979 to 1987 for regions within 200 km of significant water bodies (dark shading), and times when monthly average daytime air temperature is greater than −2 °C (light shading).

−2 °C, and SWE values above 100 mm, results in an unbiased SWE estimate with seasonal maximum 20 mm RMS median error when comparing pixels with 5 or more stations. Imposing these rules on the SMMR SWE product makes it useful for practical applications.

Acknowledgements

The authors wish to thank Jim Foster, Richard Kelly, and Hugh Powell for helpful discussions during the course of this work. This work was funded by the National

Aeronautics and Space Administration Earth Observing System Interdisciplinary Science (NASA EOS/IDS) Program NRA-99-OES-04.

References

Bellerby, T., Taberner, M., Wilmshurst, A., Beaumont, M., Barrett, E., Scott, J., et al. (1998). Retrieval of land and sea brightness temperatures from mixed coastal pixels in passive microwave data. *IEEE Transactions on Geoscience and Remote Sensing*, *36*(6), 1844–1851.

Brown, R. D. (1996). Evaluation of methods for climatological reconstruction of snow depth and snow cover duration at Canadian meteorological stations. *Proc. Eastern Snow Conf., 53d Annual Meeting* (pp. 55–65) Williamsburg, VA.

Brown, R. D. (2000). Northern hemisphere snow cover variability and change, 1915–97. *Journal of Climate*, *13*, 2339–2355.

Brown, R. D., & Braaten, R. O. (1998). Spatial and temporal variability of Canadian monthly snow depths, 1946–1995. *Atmosphere-Ocean*, *36*(1), 37–54.

Brown, R. D., Brasnett, B., & Robinson, D. (2003). Gridded North American monthly snow depth and snow water equivalent for GCM evaluation. *Atmosphere-Ocean*, *41*(1), 1–14.

Chang, A. T. C., Foster, J. L., & Hall, D. K. (1996). Effects of forest on the snow parameters derived from microwave measurements during the BOREAS winter field experiment. *Hydrological Processes*, *10*, 1565–1574.

Chang, A. T. C., Foster, J. L., & Hall, D. K. (1987). Nimbus-7 derived global snow cover parameters. *Annals of Glaciology*, *9*, 39–44.

Chang, A. T. C., Kelly, R. E., Josberger, E. G., Armstrong, R. L., Foster, J. L., & Mognard, N. M. (2005). Analysis of ground-measured and passive-microwave-derived snow depth variations in midwinter across the northern Great Plains. *Journal of Hydrometeorology*, *6*(1), 20–33.

Cohen, J. (1994). Snow cover and climate. *Weather*, *49*, 150–155.

Cohen, J., & Entekhabi, D. (1999). Eurasian snow cover variability and Northern Hemisphere climate predictability. *Geophysical Research Letters*, *26*, 345–348.

Delworth, T. L., & Manabe, S. (1998). The influence of potential evaporation on variabilities of simulated soil wetness and climate. *Journal of Climate*, *1*, 523–547.

Derksen, C., LeDrew, E., Walker, A., & Goodison, B. (2000). The influence of sensor overpass time on passive microwave retrieval of snow cover parameters. *Remote Sensing of Environment*, *73*(3), 297–308.

Dong, J., Kaufmann, R. K., Myneni, R. B., Tucker, C. J., Kauppi, P. E., Liski, J., et al. (2003). Remote sensing of boreal and temperate forest woody biomass: Carbon pools, sources and sinks. *Remote Sensing of Environment*, *84*, 393–410.

Foster, J. L., Sun, C., Walker, J. P., Kelly, R. E. J., Chang, A. T. C., Dong, J., et al. (2005). Quantify the uncertainty in passive microwave snow water equivalent observations. *Remote Sensing of Environment*, *94*(2), 187–203.

Gesch, D. B., & Larson, K. S. (1996). Techniques for development of global 1-kilometer digital elevation models. *Pecora thirteen, human interactions with the environment-perspectives from space* (pp. 677–703). South Dakota: Sioux Falls.

Grody, N. C., & Basist, A. N. (1997). Interpretation of SSM/I measurements over Greenland. *IEEE Transactions on Geoscience and Remote Sensing*, *35*, 360–366.

Hall, D. K. (1998). Remote sensing of snow and ice using imaging radar. *Manual of remote sensing* (3rd edition) (pp. 677–703). Falls Church, VA: American Society for Photogrammetry and Remote Sensing.

Hall, D. K., Kelly, R. E. J., Riggs, G. A., Chang, A. T. C., & Foster, J. L. (2002). Assessment of the relative accuracy of hemispheric-scale snow-cover maps. *Annals of Glaciology*, *34*, 24–30.

Josberger, E. G., & Mognard, N. M. (2002). A passive microwave snow depth algorithm with a proxy for snow metamorphism. *Hydrological Processes*, *16*, 1557–1568.

Loveland, T. R., Reed, B. C., Brown, J. F., Ohler, D. O., Zhu, J., Yang, L., et al. (2000). Development of a global land cover characteristics dataset. *International Journal of Remote Sensing*, *21*, 1303–1330.

Madrid, C. R. (1978). *The Nimbus 7 user's guide, Landsat/Nimbus project*. Greenbelt, MD, USA: Goddard Space Flight Center.

Matzler, C., & Standley, A. (2000). Relief effects for passive microwave remote sensing. *International Journal of Remote Sensing*, *21*, 2403–2412.

Mote, T. L., Grundstein, A. J., Leathers, D. J., & Robinson, D. A. (2003). A comparison of modeled, remotely sensed, and measured snow water equivalent in the northern Great Plains. *Water Resource Research*, *39*(8), 1209.

New, M., Hulme, M., & Jones, P. (2000). Representing twentieth-century space-time climate variability: Part II. Development of 1901–96 monthly grids of terrestrial surface climate. *Journal of Climate*, *13*(13), 2217–2238.

Njoku, E. (1996). *Nimbus-7 SMMR pathfinder brightness temperatures*. Boulder, CO: National Snow and Ice Data Center.

Robinson, D. A., Dewey, K. F., & Heim, R. R. (1993). Global snow cover monitoring: An update. *Bulletin of American Meteorological Society*, *74*, 1689–1696.

Shukla, J., & Mintz, Y. (1982). The influence of land-surface evapotranspiration on the earth's climate. *Science*, *214*, 1498–1501.

Sturm, M., Holmgren, J., & Liston, G. E. (1995). A seasonal snow cover classification system for local to regional applications. *Journal of Climate*, *8*, 1261–1283.

Tait, A., & Armstrong, R. (1996). Evaluation of SMMR satellite-derived snow depth using ground-based measurements. *International Journal of Remote Sensing*, *17*, 657–665.

Ulaby, F. T., & Stiles, W. H. (1980). Microwave radiometric observations of snow packs, NASA CP-2153. *NASA workshop on the microwave remote sensing of snow pack properties* (pp. 187–201). Ft. Collins, CO.

West, R. D., Winebrenner, D. P., Tsang, L., & Rott, H. (1996). Microwave emission from density-stratified Antarctic firn at 6 cm wavelength. *Journal of Glaciology*, *42*, 63–76.

Yang, F., Kumar, A., Wang, W., Juang, H. H., & Kanamitsu, M. (2001). Snow-albedo feedback and seasonal climate variability over North America. *Journal of Climate*, *14*, 4245–4248.